



# On-board reforming of biodiesel and bioethanol for high temperature PEM fuel cells: Comparison of autothermal reforming and steam reforming

Stefan Martin\*, Antje Wörner

German Aerospace Center, Institute of Technical Thermodynamics Pfaffenwaldring 38-40, 70569 Stuttgart, Germany

## ARTICLE INFO

### Article history:

Received 17 August 2010  
Received in revised form  
18 November 2010  
Accepted 20 November 2010  
Available online 27 November 2010

### Keywords:

Hydrogen, On-board fuel processor,  
Biodiesel, Bioethanol, PEM fuel cell,  
Reforming

## ABSTRACT

In the 21st century biofuels will play an important role as alternative fuels in the transportation sector. In this paper different reforming options (steam reforming (SR) and autothermal reforming (ATR)) for the on-board conversion of bioethanol and biodiesel into a hydrogen-rich gas suitable for high temperature PEM (HTPEM) fuel cells are investigated using the simulation tool Aspen Plus. Special emphasis is placed on thermal heat integration. Methyl-oleate ( $C_{19}H_{36}O_2$ ) is chosen as reference substance for biodiesel. Bioethanol is represented by ethanol ( $C_2H_5OH$ ). For the steam reforming concept with heat integration a maximum fuel processing efficiency of 75.6% (76.3%) is obtained for biodiesel (bioethanol) at  $S/C = 3$ . For the autothermal reforming concept with heat integration a maximum fuel processing efficiency of 74.1% (75.1%) is obtained for biodiesel (bioethanol) at  $S/C = 2$  and  $\lambda = 0.36$  (0.35). Taking into account the better dynamic behaviour and lower system complexity of the reforming concept based on ATR, autothermal reforming in combination with a water gas shift reactor is considered as the preferred option for on-board reforming of biodiesel and bioethanol. Based on the simulation results optimum operating conditions for a novel 5 kW biofuel processor are derived.

© 2010 Elsevier B.V. All rights reserved.

## 1. Introduction

Today there is great interest in developing fuel cell systems for the transportation sector. Fuel cells are considered as a promising, environmental-friendly option for powering future cars and auxiliary power units (APU) for all kinds of vehicles. Polymer electrolyte membrane (PEM) fuel cells are considered as the most promising option for transportation applications because of their high power density which is an order of magnitude higher than for any other type of fuel cell [1]. The operating temperatures are typically between 70 and 90 °C. In order to avoid poisoning of the platinum electrode the CO concentration in the feed gas has to be reduced below 20 ppm [2].

This paper focuses on hydrogen production from biofuels for high temperature PEM (HTPEM) fuel cells. HTPEM fuel cells are operated at slightly higher inlet temperatures of 120–180 °C [3]. Li et al. reported that a HTPEM based on polybenzimidazoles, a high-temperature polymer which has been firstly synthesized by Carl Shipp Marvel in the 1960s, can tolerate up to 1 Vol.-% CO and 10 ppm  $SO_2$  in the fuel stream, allowing for simplification of the fuel processing system [4]. Thus it is possible to reach the CO requirements for a HTPEM by using only a water gas shift stage.

As there is no existing infrastructure for hydrogen available, the feed hydrogen for high temperature PEM fuel cells has to be supplied by on-board reforming of existing transportation fuels such as gasoline, diesel and biofuels [2]. Especially liquid biofuels have recently attracted increasing attention as alternative sources for the transportation sector [5]. Demirbas comes to the conclusion that bioethanol and biodiesel are the two liquid transportation fuels with the highest potential to replace gasoline and diesel fuel in the future [6]. Currently, bioethanol which is derived mainly by fermentation of sugar cane and starch is by far the most widespread non-fossil alternative fuel in the world. World production of bioethanol increased from 24.5 million metric tons in the year 2004 to 60 million metric tons in 2009 [7]. This is about 4% of the worldwide gasoline consumption. World production of biodiesel, a synthetic diesel-like fuel produced by transesterification of vegetable oils, increased from 2 million metric tons in the year 2004 to 15 million metric tons in 2009. This accounts for approximately 0.2% of diesel consumed for transport [6].

In a first step the liquid biofuels have to be converted into a hydrogen-rich gas by the means of reforming. Steam reforming (SR) is the most widely practiced commercial process for hydrogen and synthesis gas production [8]. It is well known, that SR has the highest hydrogen efficiency amongst the available reforming options [9–11]. One of the early applications of steam reforming was the catalytic synthesis of ammonia from hydrogen and atmospheric nitrogen, a process which was developed by Fritz Haber and Carl Bosch in 1909.

\* Corresponding author. Tel.: +49 711 6862 682; fax: +49 711 6862 665.  
E-mail addresses: [stefan.martin@dlr.de](mailto:stefan.martin@dlr.de) (S. Martin), [antje.woerner@dlr.de](mailto:antje.woerner@dlr.de) (A. Wörner).

If H<sub>2</sub>O is replaced by CO<sub>2</sub> (=CO<sub>2</sub> reforming, CR) a synthesis gas with a lower H<sub>2</sub>:CO ratio is obtained. By combining SR and CR a synthesis gas ideal for conventional methanol plants can be produced.

Synthesis gas can also be produced by partial oxidation of hydrocarbons with oxygen (POX). POX is divided into thermal partial oxidation (TPOX) at temperatures higher than 1200 °C being used for sulphur-containing heavy hydrocarbon fuels and catalytic partial oxidation (CPOX) for low-sulphur feedstock taking place at temperatures of 900–1000 °C.

Autothermal reforming (ATR) is a mixture of SR and POX using steam and oxygen to produce a hydrogen rich synthesis gas. In order to obtain pure hydrogen from the reformat gas of either SR, CR, POX or ATR (with subsequent water gas shift) further gas purification steps are necessary, e.g., preferential methanation, preferential oxidation and pressure swing adsorption [8,12].

Ersoz et al. [13] compared SR, ATR and POX for a combined reformer PEM fuel cell system using natural gas, gasoline and diesel as hydrocarbon sources. They come to the conclusion that steam reforming and autothermal reforming appear as the most competitive options in terms of fuel processor efficiency for PEM fuel cells.

Giunta et al. [14] analyzed hydrogen production from steam reforming for PEM fuel cells using bioethanol as raw material. They conclude that hydrogen production using ethanol as raw material is a very attractive alternative to those technologies based on fossil fuels.

Ersoz et al. [15] studied the performance of autothermal reforming for two different hydrocarbon mixtures. The results indicate very similar behaviour for both of the investigated fuels. The maximum fuel processing efficiency is reported at  $T = 700$  °C.

Benito et al. [16] performed extensive thermodynamic analysis of a 1 kW bioethanol steam reforming processor for PEMFC operation. A processor efficiency of 73.7% for S/C = 3.2 was achieved taking advantage of the heat released in the exothermic stages. By using the energy content of the unconverted hydrogen of the exhaust anode gas stream an energy efficiency of the processor-fuel cell system of 30% was achieved.

The objective of this article is to evaluate different reforming concepts for on-board reforming of biodiesel and bioethanol for use with high temperature PEM fuel cells in the transportation sector, e.g., APU applications for cars, trucks and ships. Conversion of biodiesel and bioethanol into a hydrogen-rich gas is analyzed with the simulation tool Aspen Plus. Two different reforming options (SR and ATR) are compared in terms of hydrogen efficiency, fuel processing efficiency, dynamic behaviour, product gas composition, system complexity and sulphur resistance. An extensive parameter study is carried out in order to find optimum operating conditions for a 5 kW biofuel processor suitable for HTPM applications. As on-board reforming of liquid biofuels requires compact, low-volume, low-weight reformers the approach within this work was to keep the system as simple as possible, using only waste heat streams from within the system to preheat air, water and fuel. An elaborated thermal heat integration system is set up for both reforming concepts to achieve high preheating temperatures and thus a high overall system efficiency.

## 2. Methodology

### 2.1. Bioethanol and biodiesel

In this work bioethanol is represented by pure ethanol C<sub>2</sub>H<sub>5</sub>OH. Analysis of biodiesel was performed with a commercial GC-FID system. Based on the analysis methyl-oleate (C<sub>19</sub>H<sub>36</sub>O<sub>2</sub>) was chosen as a reference substance for biodiesel. Methyl-oleate is derived by transesterification of triolein, the triglyceride of oleic acid, which

**Table 1**

Physical and chemical properties of biodiesel and model substance methyl-oleate (C<sub>19</sub>H<sub>36</sub>O<sub>2</sub>).

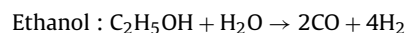
|                                                        | Biodiesel | Methyl-oleate |
|--------------------------------------------------------|-----------|---------------|
| Molecular weight (g mol <sup>-1</sup> )                | 295.2     | 296.5         |
| Mass density at $T = 15$ °C (kg m <sup>-3</sup> )      | 878.0     | 872.0         |
| Sulphur content (ppmw)                                 | 3.3       | 0             |
| Lower heating value (kJ kg <sup>-1</sup> )             | 37,790    | 37,438        |
| Kinematic viscosity (mm <sup>2</sup> s <sup>-1</sup> ) | 4.08      | 7.8           |
| O <sub>2</sub> -content (% by weight)                  | 10.8      | 10.7          |

is the dominating fatty acid of rapeseed oil. In Table 1 the chemical and physical properties of biodiesel are compared with those of the model substance methyl-oleate (C<sub>19</sub>H<sub>36</sub>O<sub>2</sub>). As can be seen there are only small differences.

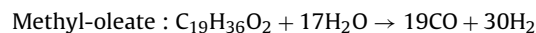
### 2.2. Chemical reaction system

Reforming of bioethanol and methyl-oleate (model substance for biodiesel) involves the following chemical reactions (please notice that the reaction enthalpies  $\Delta H$  refer to  $T = 700$  °C, which is typical for reforming of liquid fuels) [1]:

a) Steam reforming

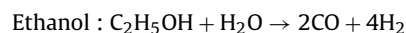


$$\Delta H_{973\text{K}} = +278.5 \text{ kJ/mol} \quad (1)$$

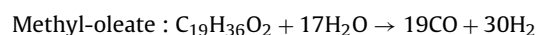
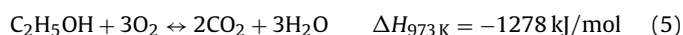


$$\Delta H_{973\text{K}} = +2701 \text{ kJ/mol} \quad (2)$$

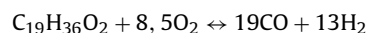
b) Autothermal reforming



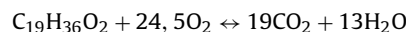
$$\Delta H_{973\text{K}} = +278.5 \text{ kJ/mol} \quad (3)$$



$$\Delta H_{973\text{K}} = +2701 \text{ kJ/mol} \quad (6)$$



$$\Delta H_{973\text{K}} = -1512 \text{ kJ/mol} \quad (7)$$



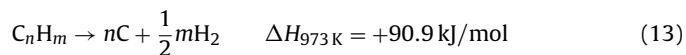
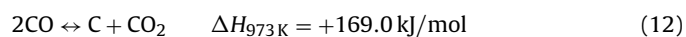
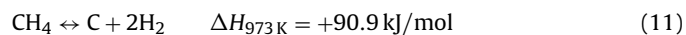
$$\Delta H_{973\text{K}} = -10,107 \text{ kJ/mol} \quad (8)$$

Parallel to the steam reforming and autothermal reforming reactions methanation (Eq. (9)) and water gas shift reaction (Eq. (10)) take place:



Steam reforming is an endothermic reaction, thus being favoured at high reforming temperatures while water gas shift and methanation are exothermic reactions being favoured at low temperatures. In order to achieve a maximum hydrogen output the water gas shift reactor is commonly operated separately from the reformer at lower temperatures.

In addition to these main reforming reactions, unwanted side reactions can take place which might lead to carbon formation (Eqs. (11)–(13)). The extent of these undesired side reactions strongly depends on reaction kinetics and reformer operating conditions (temperature, steam to carbon ratio, air ratio, type of catalyst) [17].



### 2.3. Implementation of reforming concepts into Aspen Plus

Reforming of bioethanol and biodiesel for HTPeM applications was studied using the simulation tool Aspen Plus which is widely used in industry and academia today. For university students and teachers a special University Package for process engineering is available.<sup>1</sup> Aspen Plus stores physical property parameters for a large number of components in several databanks. Based on an appropriate selection of a thermodynamic property method Aspen uses mathematical models to predict the performance of the process. Each property method in the Aspen physical property system is based on either an equation-of-state method or an activity coefficient method for phase equilibrium calculations. The phase equilibrium method determines how other thermodynamic properties such as enthalpies and molar volumes are calculated. Besides chemical reaction equilibrium can be calculated by minimizing the free Gibbs energy. Kinetic limitations of chemical reactions can be taken into account by specifying a temperature approach. Within this paper all calculations are based on thermodynamic equilibrium conditions in the reformer outlet gas. This assumption is justified for high outlet temperatures and low space velocities. For the evaluation of the steam reforming concept and the autothermal reforming concept  $\text{H}_2$ ,  $\text{CO}$ ,  $\text{CO}_2$ ,  $\text{CH}_4$ ,  $\text{H}_2\text{O}$ ,  $\text{N}_2$ ,  $\text{C}_2\text{H}_6$ ,  $\text{C}_2\text{H}_4$ ,  $\text{C}_3\text{H}_8$  and unconverted liquid fuel are specified as possible products.

#### 2.3.1. Steam reforming concept

The steam reforming concept implemented in Aspen Plus consists of an isothermal steam reformer, a burner, a water–gas-shift reactor and further auxiliary system components (Figs. 1 and 2). The reforming reactor is fed with preheated steam ( $\text{H}_2\text{O}$ -REF) and fuel (FUEL-REF). The steam reforming product gas temperature  $T_{\text{SR-OUT}}$  is adjusted by the heat  $\dot{Q}$  – SR which is released by burning part of the fuel in a combustion chamber. The fluegas (FLUEGAS) is cooled down to 180 °C. After leaving the reforming reactor the reformate gas stream (SR-OUT) is cooled down by the water gas shift inlet temperature  $T_{\text{WGS-IN}} = 250$  °C. Additional gas cleaning units, e.g., preferential oxidation or methanation, are not necessary. After leaving the water gas shift reactor the gas is further cooled down to the HTPeM inlet temperature  $T_{\text{BZ-IN}} = 160$  °C.

In order to achieve high overall system efficiency a sophisticated thermal heat integration system was set up for the steam reforming concept (Fig. 2). The idea of the system with heat integration is to fully use the internal waste heat streams for preheating  $\text{H}_2\text{O}$ -SR, FUEL-SR and AIR and to meet the energy demand for the endothermic steam reforming reactions. By cooling down the product gas stream SR-OUT to the water gas shift inlet temperature  $T_{\text{WGS-IN}} = 250$  °C the incoming water  $\text{H}_2\text{O}$ -1 is preheated. The enthalpy of the burner offgas (FLUEGAS) is used to preheat AIR-1 (W2), fully evaporate  $\text{H}_2\text{O}$ -2 (W3), overheat  $\text{H}_2\text{O}$ -3 (W4) and preheat FUEL-SR1. The outlet temperature  $T_{\text{FLUE-OUT}}$  was set to 180 °C which is considered as a realistic value for compact reformers.

The operating conditions used for simulation in Aspen Plus for the reforming concept based on steam reforming can be summarized as follows:

- Reactor type: Gibbs (thermodynamic equilibrium conditions).
- Reformer: isothermal.
- Product gas temperature  $T_{\text{SR-OUT}}$ : adjusted by burning part of the fuel (temperature is varied between 550 and 850 °C, see Figs. 5 and 7).
- Feed temperatures: a) system without heat integration (Fig. 1):  $T_{\text{H}_2\text{O-SR}}$ ,  $T_{\text{FUEL-SR}}$ ,  $T_{\text{AIR}}$ : 25 °C, three different preheating temperatures realized for  $T_{\text{H}_2\text{O-REF}}$  and  $T_{\text{AIR-B}}$ , see Fig. 5; b) thermally integrated system (Fig. 2):  $T_{\text{H}_2\text{O-SR}}$ ,  $T_{\text{FUEL-SR}}$  and  $T_{\text{AIR}}$ : 25 °C;  $\text{H}_2\text{O}$ -SR and FUEL-SR are preheated to  $T_{\text{H}_2\text{O-REF}}$  and  $T_{\text{FUEL-REF}}$ . AIR is preheated to  $T_{\text{AIR-B}}$ .
- Minimum temperature approach for counter current heat exchangers:  $\Delta T = 20$  K.

The following parameters were kept constant during simulation:  $T_{\text{WGS}}$ : 250 °C;  $p$ : atmospheric; steam to carbon-ratio: 3;  $T_{\text{BZ-IN}}$ : 160 °C;  $T_{\text{FLUE-OUT}}$ : 180 °C.

#### 2.3.2. Autothermal reforming concept

The autothermal reforming concept (Figs. 3 and 4) consists of an adiabatic ATR reformer, a water–gas-shift reactor and further auxiliary system components. Biodiesel and bioethanol are converted into a hydrogen-rich product gas (ATR-OUT) by adding preheated air (AIR-REF) and steam ( $\text{H}_2\text{O}$ -REF). At a given feed mole flow and a constant steam to carbon ratio the equilibrium reformate gas temperature depends directly from the amount of air added. After leaving the ATR-reactor the reformate gas stream (ATR-OUT) is cooled down to the water gas shift inlet temperature  $T_{\text{WGS-IN}} = 250$  °C. Additional gas cleaning units are not necessary as the high temperature PEM fuel cell can tolerate up to 1 Vol.-% CO [4]. After leaving the water gas shift reactor the gas is further cooled down to the HTPeM inlet temperature of 160 °C.

The idea of the thermally integrated ATR-system (Fig. 4) is to use the enthalpy of the ATR-OUT stream by cooling it down to  $T_{\text{WGS}} = 250$  °C, thereby evaporating the incoming water stream  $\text{H}_2\text{O}$ -1. Two main limitations have to be considered for the operation of the thermally integrated system based on ATR:

1. Water has to be fully evaporated before entering the ATR-reactor (Enthalpy of ATR-OUT must be high enough to fully evaporate the incoming water  $\text{H}_2\text{O}$ -1 prior to entering the ATR-reactor).
2.  $T_{\text{ATR-OUT}}$  must not exceed 1000 °C (problems with material stability might arise).

The operating conditions used for simulation in Aspen Plus for the reforming concept based on autothermal reforming can be summarized as follows:

- Reactor type: Gibbs (thermodynamic equilibrium conditions).
- Reformer: adiabatic.
- Product gas temperature  $T_{\text{ATR-OUT}}$ : dependant on amount of air (AIR-REF) fed to the reformer (air ratio is varied between 0 and 1, see Figs. 6, 8 and 9).
- Steam to carbon-ratio: 3, 2
- Feed temperatures: a) system without heat integration (Fig. 3):  $T_{\text{H}_2\text{O-ATR}}$ ,  $T_{\text{AIR-ATR}}$ ,  $T_{\text{FUEL-ATR}}$ : 25 °C (three different preheating temperatures realized for  $T_{\text{H}_2\text{O-REF}}$  and  $T_{\text{AIR-REF}}$ , see Fig. 6); b) thermally integrated system (Fig. 4):  $T_{\text{AIR-REF}}$ ,  $T_{\text{FUEL-REF}}$ : 25 °C;  $\text{H}_2\text{O}$ -ATR is preheated to  $T_{\text{H}_2\text{O-REF}} > 100$  °C.

Minimum temperature approach for counter current heat exchanger: 20 K.

<sup>1</sup> <http://www.aspentech.com/corporate/university/products.aspx>.

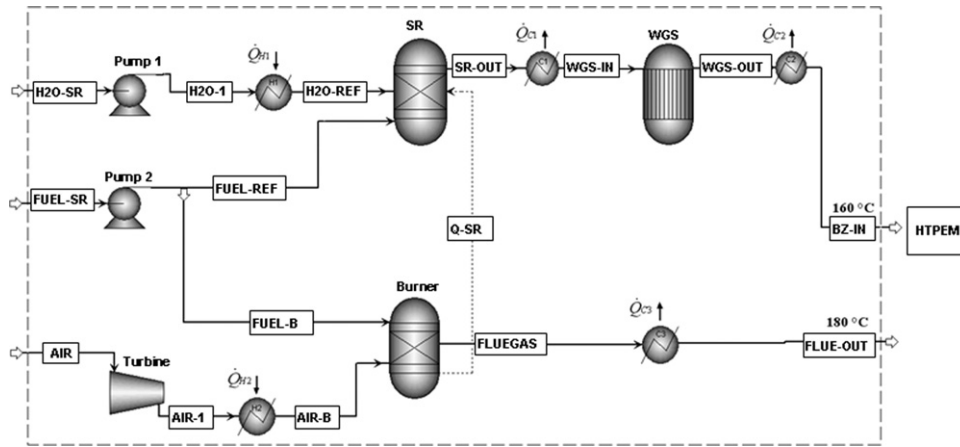


Fig. 1. Reforming concept based on steam reforming without heat integration.

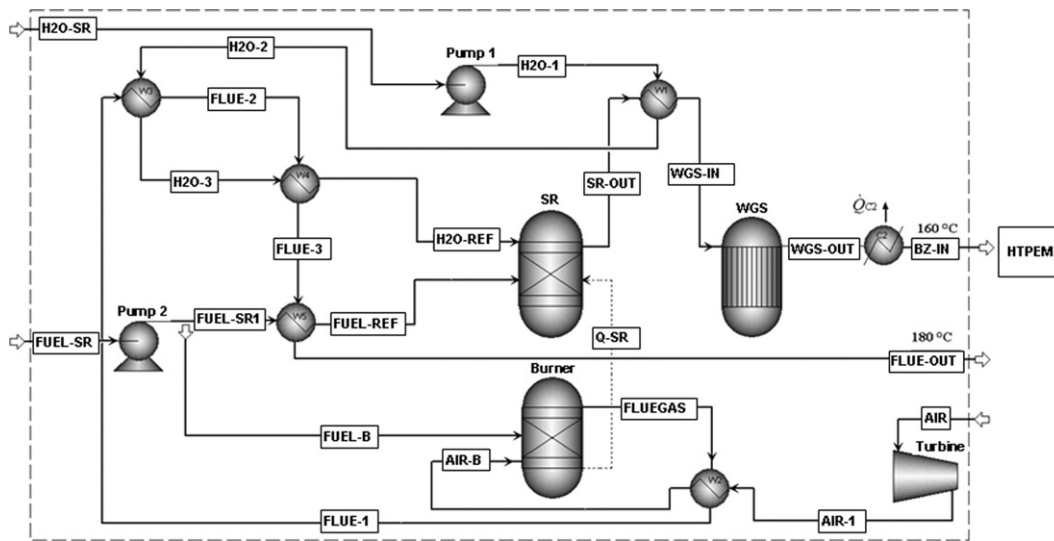


Fig. 2. Reforming concept based on steam reforming with heat integration.

The following parameters were kept constant during simulation:  $T_{WGS}$ : 250 °C;  $p$ : atmospheric;  $T_{BZ-IN}$ : 160 °C.

#### 2.4. Evaluation of reforming concepts

A common parameter for evaluating reformer concepts is the thermal hydrogen efficiency  $\eta_{H_2}$  which is defined by the relation of

the lower heating value of hydrogen in the reformat gas (BZ-IN) to the lower heating value of the fuel (FUEL-REF):

$$\eta_{H_2} = \frac{\dot{m}(H_2) \cdot LHV(H_2)}{\dot{m}(FUEL - REF) \cdot LHV(FUEL - REF)} \quad (14)$$

The steam reforming concept requires additional fuel (FUEL-B) for the burner in order to supply the necessary heat for the endothermic reforming reactions which take place at a high tem-

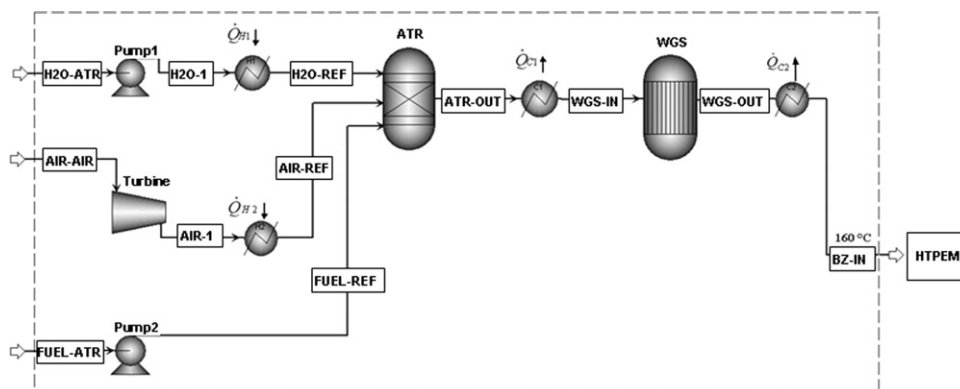


Fig. 3. Reforming concept based on autothermal reforming without heat integration.

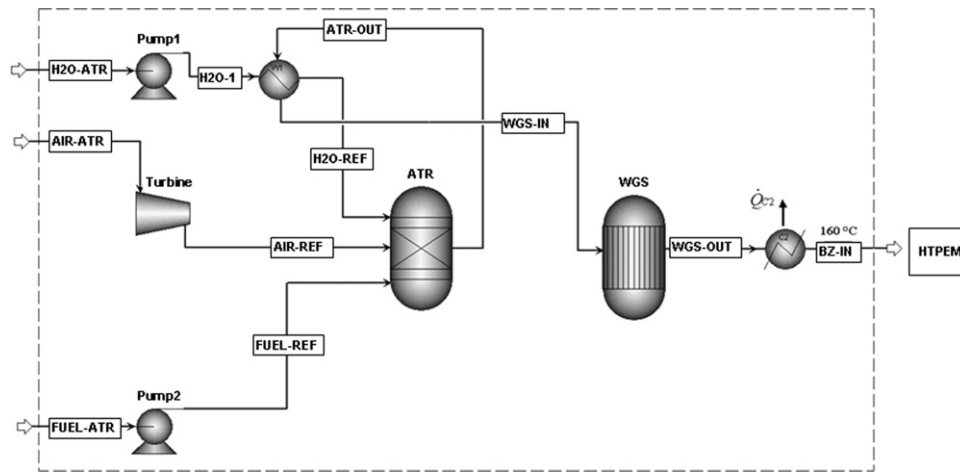


Fig. 4. Reforming concept based on autothermal reforming with heat integration.

perature level. Taking into account the additional fuel for the burner the effective hydrogen efficiency  $\eta_{H_2, \text{eff}}$  becomes:

$$\eta_{H_2, \text{eff}} = \frac{\dot{m}(H_2) \cdot \text{LHV}(H_2)}{\dot{m}(\text{FUEL} - \text{REF}) \cdot \text{LHV}(\text{FUEL} - \text{REF}) + \dot{m}(\text{FUEL} - \text{B}) \cdot \text{LHV}(\text{FUEL} - \text{B})} \quad (15)$$

The overall fuel processing efficiency  $\eta_{FP}$  which can be applied to both ATR and SR concept also considers energy demand for external heating  $\dot{Q}_{\text{heat, ext.}}$  and electrical power for auxiliary devices:

$$\eta_{FP} = \frac{\dot{m}(H_2) \cdot \text{LHV}(H_2)}{\dot{m}(\text{FUEL}_{\text{total}}) \cdot \text{LHV}(\text{FUEL}_{\text{total}}) + \dot{Q}_{\text{heat, ext.}} + P_{\text{el}}} \quad (16)$$

The overall system efficiency  $\eta_{\text{system}}$  is calculated by multiplying the fuel processing efficiency  $\eta_{FP}$  with the fuel cell efficiency  $\eta_{FC}$ :

$$\eta_{\text{system}} = \eta_{FP} \cdot \eta_{FC} \quad (17)$$

### 3. Results and discussion

#### 3.1. Hydrogen efficiency without heat integration

For the steam reforming concept without considering heat integration (Fig. 1) hydrogen efficiency  $\eta_{H_2}$  and effective hydrogen efficiency  $\eta_{H_2, \text{eff}}$  were calculated in the temperature range 550–850 °C. The influence of preheating  $H_2O$ -REF and AIR-B on hydrogen efficiency was investigated. Analogue simulations have been conducted for the autothermal reforming concept (Fig. 3). Hydrogen efficiency  $\eta_{H_2}$  was calculated for different preheating temperatures of  $T_{H_2O\text{-REF}}$  and  $T_{\text{AIR-REF}}$  with air ratios ranging from 0 to 1.

##### 3.1.1. Steam reforming concept

Fig. 5 shows the effect of preheating water ( $H_2O$ -REF) and combustion air (AIR-B) on hydrogen efficiency  $\eta_{H_2}$  and effective hydrogen efficiency  $\eta_{H_2, \text{eff}}$ . Preheating obviously has no effect on hydrogen efficiency  $\eta_{H_2}$  as only the amount of fuel needed for the reformer is considered for calculating  $\eta_{H_2}$  (Eq. (14)). A maximum hydrogen efficiency of 116% for biodiesel and 117% for bioethanol, respectively, is obtained. The high values of hydrogen efficiency (>100%) can be explained by the fact that the overall steam reforming reaction is endothermic. For high steam to carbon ratios the lower heating value of the hydrogen output is higher than the lower heating value of the feed.

The hydrogen efficiency decreases drastically when taking into account the fuel needed for the burner in order to provide the necessary heat for the endothermic reforming reactions (see effective hydrogen efficiency  $\eta_{H_2, \text{eff}}$ , Eq. (15)). In this case preheating has a

positive effect on the effective hydrogen efficiency  $\eta_{H_2, \text{eff}}$ . For high preheating temperatures of  $T_{H_2O\text{-REF}} = 400^\circ\text{C}$  and  $T_{\text{AIR-B}} = 600^\circ\text{C}$  a maximum effective hydrogen efficiency  $\eta_{H_2, \text{eff}}$  of 81.4% is obtained for biodiesel. Using bioethanol as feed a maximum effective hydrogen efficiency  $\eta_{H_2, \text{eff}}$  of 80.4% is obtained. By preheating water and combustion air less fuel is needed for the external burner in order to supply heat for a desired steam reforming temperature  $T_{\text{SR-OUT}}$ .

It has to be kept in mind that the hydrogen efficiency  $\eta_{H_2}$  as well as the effective hydrogen efficiency  $\eta_{H_2, \text{eff}}$  are only adequate parameters for the evaluation of a reforming concept in the following two cases:

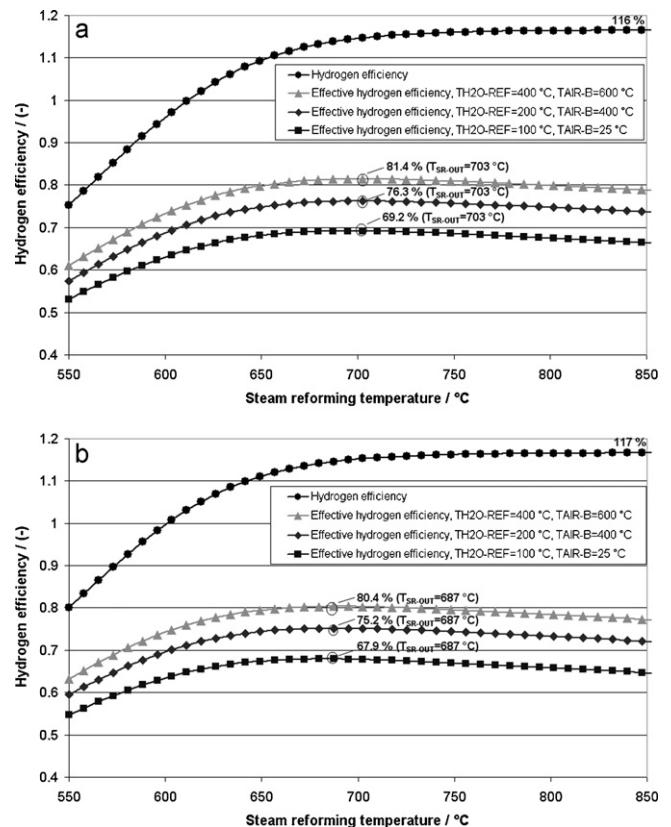


Fig. 5. Hydrogen efficiency and effective hydrogen efficiency for different preheating temperatures of  $H_2O$ -REF and AIR-B (a: biodiesel, b: bioethanol), S/C = 3.

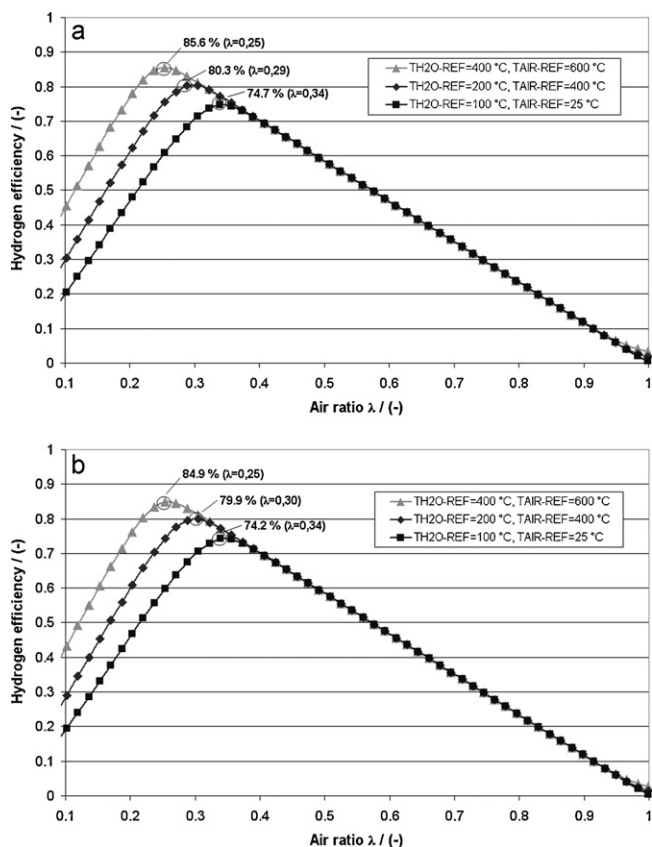


Fig. 6. Hydrogen efficiency for different preheating temperatures of  $H_2O$ -REF and AIR-REF (a: biodiesel, b: bioethanol),  $S/C=3$ .

- Waste heat is available from other processes on a high temperature level (i.e., industrial processes, solar power enhanced reforming).
- Process heat demand for desired preheating temperatures can be completely met by using internal heat streams.

This requirement can be met in large industrial plants, where waste heat from other chemical processes is available [9]. For small reformer systems, like APU applications in the transportation sector, the situation is very different. As there is often not enough waste heat available thermal heat integration is a decisive factor to achieve high preheating temperatures and thus high overall fuel processing efficiencies  $\eta_{FP}$ .

### 3.1.2. Autothermal reforming concept

Hydrogen efficiency  $\eta_{H_2}$  shows a maximum for  $\lambda_{opt}$  (Fig. 6). The maximum hydrogen efficiency  $\eta_{H_2,max}$  increases with increasing preheating of  $H_2O$ -REF and AIR-REF while the air ratio  $\lambda$  decreases at the same time. Thus, preheating of fuel and air has a positive effect on hydrogen efficiency. By preheating fuel and air less fuel has to be partially oxidized in the adiabatic ATR-reactor in order to supply the necessary heat for the endothermic reforming reactions. This results in lower air ratios. Regarding to hydrogen efficiency  $\eta_{H_2}$  there are only minor differences between biodiesel and bioethanol. This is in line with Ersoz et al. [15] who found only minor differences between different hydrocarbon mixtures used as feedstock for autothermal reforming. The positive effect of preheating feed water and feed air is limited to air ratios smaller than  $\lambda_{opt}$ . At a higher air ratio beyond  $\lambda_{opt}$  the oxidation of hydrogen dominates which leads to a decrease of the hydrogen efficiency.

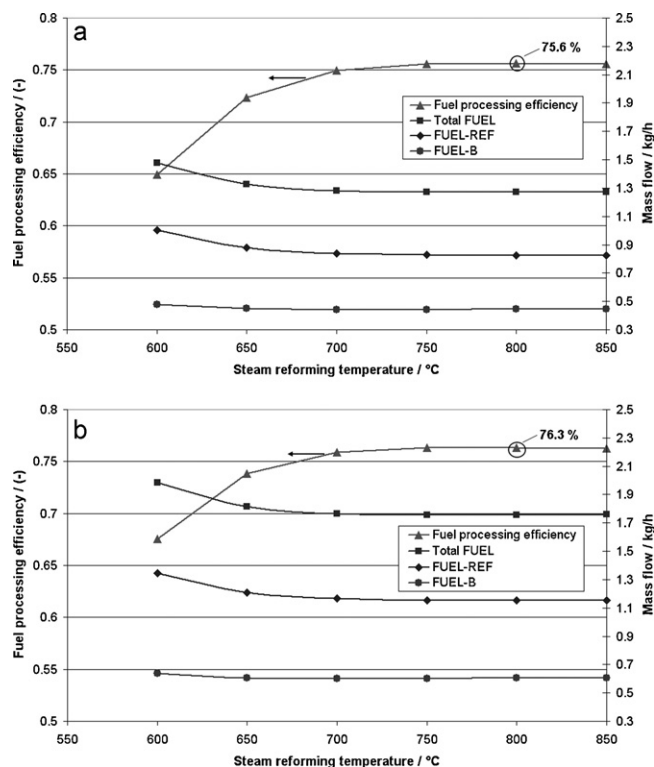


Fig. 7. Fuel processing efficiency and fuel consumption of a 5 kW biofuel processor based on steam reforming with heat integration (see Fig. 2),  $S/C=3$  (a: biodiesel, b: bioethanol).

### 3.2. Fuel processing efficiency with heat integration

For the steam reforming concept with heat integration (Fig. 2) the temperature  $T_{SR-OUT}$  is varied between 600 and 850 °C at a constant  $S/C$  ratio of 3 which is considered high enough to prevent carbon formation [18]. The resulting effects on fuel processing efficiency  $\eta_{FP}$  and fuel consumption are investigated both for biodiesel and bioethanol (Fig. 7). Analogue calculations have been carried out for the autothermal reforming concept with heat integration (Fig. 4). The influence of varying air ratio and  $S/C$  on fuel processing efficiency  $\eta_{FP}$ , amount of fuel needed ( $\dot{m}_{FUEL-REF}$ ) and product gas temperature  $T_{ATR-OUT}$  is investigated (Figs. 8 and 9).

#### 3.2.1. Steam reforming

For steam reforming temperatures higher than 700 °C, fuel processing efficiency  $\eta_{FP}$  reaches a plateau (Fig. 7). It decreases sharply when steam reforming temperatures  $T_{SR-OUT}$  fall below 700 °C. This is accompanied by an increasing amount of fuel needed for the reformer (FUEL-REF) and the burner (FUEL-B). Thus, stable operating conditions with high fuel processing efficiencies of around 76% can be ensured in a temperature range of 700–850 °C. There are only minor differences between the optimum fuel processing efficiency  $\eta_{FP}$  for biodiesel and bioethanol (75.6% versus 76.3%).

#### 3.2.2. Autothermal reforming

Considering a steam to carbon ratio of 3 the maximum fuel processing efficiency  $\eta_{FP}$  of the ATR-reformer concept being operated with bioethanol is slightly higher than with biodiesel (67.0% versus 65.7%, see Figs. 8a, 9a). At the same time more fuel is needed when using bioethanol as feed which can be explained by its lower heating value. For the operation of such a heat integrated system it is decisive to increase the air ratio  $\lambda$  beyond a minimum value  $\lambda_{min}$  which guarantees complete evaporation of water prior to entering the reformer. Furthermore it has to be ensured that the air

ratio does not exceed a maximum value  $\lambda_{max}$  which corresponds to  $T_{ATR-OUT} > 1000^\circ\text{C}$ , as problems with material stability might arise. Accordingly, for the ATR-reformer concept the air ratio must be kept between  $\lambda_{min}$  and  $\lambda_{max}$  (Figs. 8 and 9).

Using bioethanol as feed for the reformer results in slightly lower product gas temperatures  $T_{ATR-OUT}$ . This is advantageous in

terms of material stability and reduces coking risk. By decreasing the steam to carbon ratio from 3 to 2, which is supposed to be high enough to prevent coking [16], the fuel processing efficiency  $\eta_{FP}$  can be enhanced significantly (biodiesel: from 65.7% to 74.1%; bioethanol: from 67.0% to 75.1%, see Figs. 8b, 9b). This can be explained by the fact that less energy is needed to evaporate the incoming water. On the other hand increasing the S/C-ratio has a positive effect on hydrogen output of the reformat gas. These diverging effects result in an optimum S/C-ratio for heat integrated reformer systems. This is also indicated by Ioannides [19] who investigated the influence of S/C-ratio on hydrogen yield for autothermal ethanol reforming. Results show increasing hydrogen yields with decreasing S/C-ratios until an optimum S/C-ratio is reached. He found an optimum hydrogen yield of  $4.505 \text{ mol H}_2 \text{ mol}^{-1} \text{ EtOH}$  for  $S/C = 1.35$  and  $T = 694^\circ\text{C}$ . In this work the S/C-ratio was not decreased below a value of 2 in order to ensure coking free operating conditions. Additional positive effects of decreasing the S/C-ratio on system behaviour are:

- Lower fuel consumption ( $\rightarrow$  smaller fuel pump, less energy needed).
- Lower ATR-OUT temperatures ( $\rightarrow$  reduced risk of coking).
- Broader range of  $\lambda_{min} - \lambda_{max}$  ( $\rightarrow$  stable operating conditions).

### 3.3. Optimum operating conditions for a 5 kW biofuel processor

#### 3.3.1. Steam reforming concept

Tables 2 and 3 show the optimum operating conditions in terms of maximum fuel processing efficiency  $\eta_{FP}$  for a 5 kW SR fuel processor (suitable size for car/truck APU) for biodiesel and bioethanol appropriate for HTPEM-applications:

Fig. 10 shows the product gas composition at optimum operating conditions for the steam reforming concept.

Regarding the optimum operating conditions for steam reforming there are only minor differences between biodiesel and bioethanol. Fuel consumption for bioethanol is higher than for biodiesel ( $0.711 \text{ h}^{-1}$  versus  $0.481 \text{ h}^{-1}$ ) which is mainly due to its lower heating value. In order to supply the necessary heat for the endothermic steam reforming reactions 34.1% of total biodiesel and 34.9% of total bioethanol have to be combusted in the burner. For both biodiesel and bioethanol the optimum steam reforming temperature was found to be  $800^\circ\text{C}$ . After the water gas shift reactor the product gas stream BZ-IN is supplied to the high temperature PEM fuel cell at  $T = 160^\circ\text{C}$  and CO concentrations  $< 1 \text{ Vol.-%}$  (biodiesel:  $0.5 \text{ Vol.-%}$ ; bioethanol:  $0.4 \text{ Vol.-%}$ ). The hydrogen content is 56.8% for biodiesel and 54.1% for bioethanol. As the hydrogen concentration of steam reforming is considerably higher than for autothermal

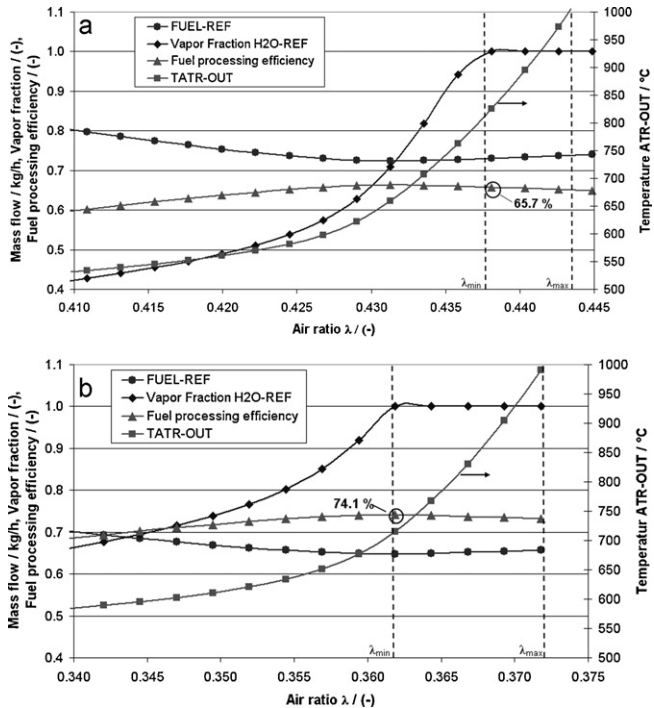


Fig. 8. Fuel processing efficiency and system behaviour of a 5 kW biodiesel fuel processor based on autothermal reforming with heat integration (see Fig. 4) (a: S/C=3, b: S/C=2).

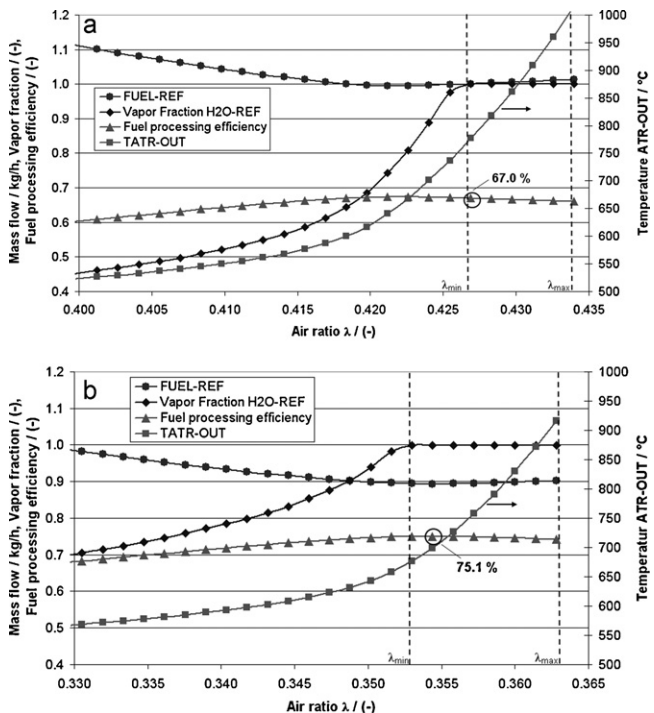


Fig. 9. Fuel processing efficiency and system behaviour of a 5 kW bioethanol fuel processor based on autothermal reforming with heat integration (see Fig. 4) (a: S/C=3, b: S/C=2).

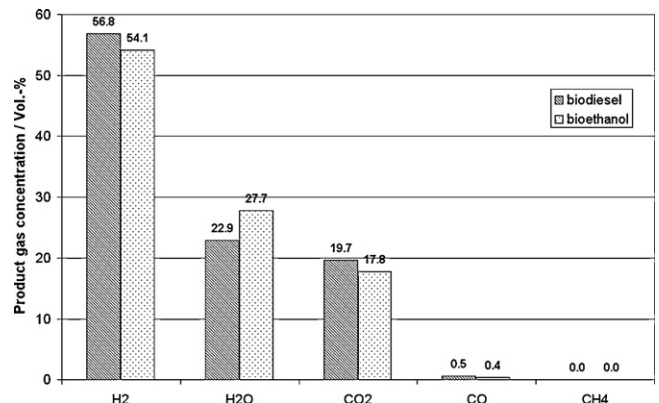


Fig. 10. Product gas composition (stream BZ-IN) at optimum operating conditions (TSR-OUT =  $800^\circ\text{C}$ ; S/C = 3).

**Table 2**Optimum operating conditions for a 5 kW biodiesel reformer based on SR concept with heat integration (see Fig. 2), S/C: 3,  $\dot{Q}$  – SR: 1.63 kW.

|                                 | H <sub>2</sub> O-SR | FUEL-SR | AIR    | H <sub>2</sub> O-REF | FUEL-REF | FUEL-B  | AIR-B | SR-OUT   |
|---------------------------------|---------------------|---------|--------|----------------------|----------|---------|-------|----------|
| $\dot{m}$ (kg h <sup>-1</sup> ) | 1.43                | 0.41    | 3.07   | 1.43                 | 0.41     | 0.22    | 3.07  | 1.84     |
| $\dot{V}$ (l h <sup>-1</sup> )  | 1.43                | 0.48    | 2625   | 3422                 | 0.49     | 0.26    | 4751  | 11,682   |
| T (°C)                          | 25                  | 25      | 25     | 350                  | 86.2     | 25      | 320   | 800      |
|                                 | FLUEGAS             | FLUE-1  | FLUE-2 | FLUE-3               | WGS-IN   | WGS-OUT | BZ-IN | FLUE-OUT |
| $\dot{m}$ (kg h <sup>-1</sup> ) | 3.29                | 3.29    | 3.29   | 3.29                 | 1.84     | 1.84    | 1.84  | 3.29     |
| $\dot{V}$ (l h <sup>-1</sup> )  | 11,063              | 9013    | 6201   | 4408                 | 5689     | 5691    | 4708  | 4270     |
| T (°C)                          | 900                 | 683     | 384    | 195                  | 250      | 250     | 160   | 180      |

**Table 3**Optimum operating conditions for a 5 kW bioethanol reformer based on SR concept with heat integration (see Fig. 2), S/C: 3,  $\dot{Q}$  – SR: 1.53 kW.

|                                 | H <sub>2</sub> O-SR | FUEL-SR | AIR    | H <sub>2</sub> O-REF | FUEL-REF | FUEL-B  | AIR-B | SR-OUT   |
|---------------------------------|---------------------|---------|--------|----------------------|----------|---------|-------|----------|
| $\dot{m}$ (kg h <sup>-1</sup> ) | 1.35                | 0.58    | 2.99   | 1.35                 | 0.58     | 0.30    | 2.99  | 1.93     |
| $\dot{V}$ (l h <sup>-1</sup> )  | 1.35                | 0.71    | 2556   | 2971                 | 378      | 0.37    | 4240  | 12,272   |
| T (°C)                          | 25                  | 25      | 25     | 300                  | 169      | 25      | 320   | 800      |
|                                 | FLUEGAS             | FLUE-1  | FLUE-2 | FLUE-3               | WGS-IN   | WGS-OUT | BZ-IN | FLUE-OUT |
| $\dot{m}$ (kg h <sup>-1</sup> ) | 3.29                | 3.29    | 3.29   | 3.29                 | 1.93     | 1.93    | 1.93  | 3.29     |
| $\dot{V}$ (l h <sup>-1</sup> )  | 11,177              | 9394    | 7443   | 6151                 | 5976     | 5978    | 4944  | 4376     |
| T (°C)                          | 900                 | 699     | 497    | 363                  | 250      | 250     | 160   | 180      |

reforming a fuel cell efficiency of 40% can be assumed [1]. In this case an overall system efficiency  $\eta_{\text{sys}}$  of 30.2% is obtained for biodiesel, respectively 30.5% for bioethanol. This is in good agreement with Benito et al. [16] who found a bioethanol processor – fuel cell system efficiency of 30%. Francesconi et al. [20] investigated a conceptual design of a bioethanol processor for PEM fuel cell applications with heat integration. They report a slightly higher overall system efficiency of 43%.

### 3.3.2. Autothermal reforming concept

Based on the simulation results the optimum operating parameters in terms of maximum fuel processing efficiency  $\eta_{\text{FP}}$  for a 5 kW ATR fuel processor running on biodiesel and bioethanol are given in Tables 4 and 5.

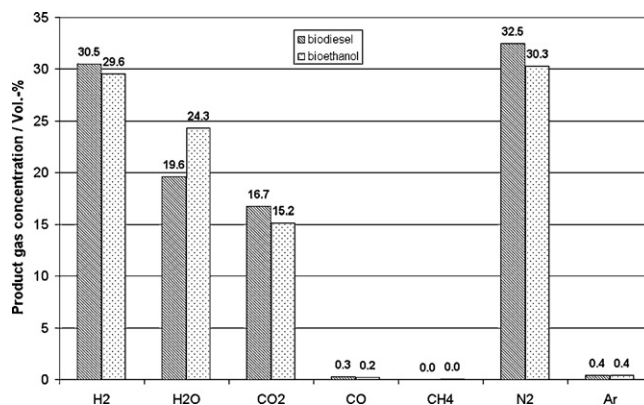
In order to convert biodiesel into a hydrogen rich gas with a maximum fuel processing efficiency  $\eta_{\text{FP, max}}$  0.75 l h<sup>-1</sup> fuel (FUEL-ATR), 1.50 l h<sup>-1</sup> water (H<sub>2</sub>O-ATR) and 2.52 m<sup>3</sup> h<sup>-1</sup> air (AIR-ATR) must be fed to the reformer. For the conversion of bioethanol the fuel consumption is somewhat higher. 1.10 l h<sup>-1</sup> fuel (FUEL-ATR), 1.40 l h<sup>-1</sup> water (H<sub>2</sub>O-ATR) and 2.43 m<sup>3</sup> h<sup>-1</sup> air (AIR-ATR) must be fed to the reformer. The optimum air ratio  $\lambda_{\text{opt}}$  is marginally lower (0.35 versus 0.36) which results in a slightly lower product gas temperature  $T_{\text{ATR-OUT}}$  (699 °C versus 715 °C). The product gas composition of stream BZ-IN which corresponds to the optimum fuel processing efficiency  $\eta_{\text{FP, max}}$  is shown in Fig. 11.

**Table 4**Optimum operating conditions for a 5 kW biodiesel reformer based on ATR concept with heat integration (see Fig. 4), air ratio  $\lambda_{\text{opt}} = 0.36$ ; S/C=2.

|                                 | H <sub>2</sub> O-ATR | AIR-ATR | FUEL-ATR | H <sub>2</sub> O-REF | AIR-REF | FUEL-REF | ATR-OUT | WGS-IN | WGS-OUT | BZ-IN |
|---------------------------------|----------------------|---------|----------|----------------------|---------|----------|---------|--------|---------|-------|
| $\dot{m}$ (kg h <sup>-1</sup> ) | 1.50                 | 2.95    | 0.65     | 1.50                 | 2.95    | 0.65     | 5.09    | 5.09   | 5.09    | 5.09  |
| $\dot{V}$ (l h <sup>-1</sup> )  | 1.50                 | 2520    | 0.75     | 2309                 | 2337    | 0.75     | 20,099  | 10,614 | 10,616  | 8782  |
| T (°C)                          | 25                   | 25      | 25       | 128                  | 31      | 25       | 715     | 250    | 250     | 160   |

**Table 5**Optimum operating conditions for a 5 kW bioethanol reformer based on ATR concept with heat integration (see Fig. 4), air ratio  $\lambda_{\text{opt}} = 0.35$ ; S/C=2.

|                                 | H <sub>2</sub> O-ATR | AIR-ATR | FUEL-ATR | H <sub>2</sub> O-REF | AIR-REF | FUEL-REF | ATR-OUT | WGS-IN | WGS-OUT | BZ-IN |
|---------------------------------|----------------------|---------|----------|----------------------|---------|----------|---------|--------|---------|-------|
| $\dot{m}$ (kg h <sup>-1</sup> ) | 1.40                 | 2.85    | 0.89     | 1.40                 | 2.85    | 0.89     | 5.14    | 5.14   | 5.14    | 5.14  |
| $\dot{V}$ (l h <sup>-1</sup> )  | 1.40                 | 2435    | 1.10     | 2658                 | 2258    | 1.10     | 20,398  | 10,958 | 10,960  | 9065  |
| T (°C)                          | 25                   | 25      | 25       | 220                  | 31      | 25       | 699     | 250    | 250     | 160   |

**Fig. 11.** Product gas composition (stream BZ-IN) at optimum operating conditions ( $\lambda_{\text{opt}}$  biodiesel: 0.36;  $\lambda_{\text{opt}}$  bioethanol: 0.35; S/C=2).

As can be seen from Fig. 11 the hydrogen concentration in the product gas stream BZ-IN is 30.5 Vol.-% for biodiesel compared to 29.6 Vol.-% for bioethanol. For connection with a high temperature PEM fuel cell stable operating conditions can be ensured as carbon monoxide concentration is decreased by water gas shift to <1 Vol.-% (0.3% for biodiesel; 0.2% for bioethanol). However, dilution with air results in a high nitrogen content (biodiesel: 32.5%; bioethanol: 30.3%) which has a negative effect on fuel cell efficiency. Consider-



ing a fuel cell efficiency of 35% an overall system efficiency  $\eta_{\text{sys}}$  of 25.9% is obtained for biodiesel, respectively 26.3% for bioethanol. This is in good agreement with Specchia et al. [21] who found a maximum net electrical efficiency of a biodiesel ATR-PEMFC system of 29%.

#### 4. Conclusions

Hydrogen production from bioethanol and biodiesel for use with HTPEM fuel cells has been studied within this paper. Extensive simulation work including a variation of reforming temperature, air ratio and steam to carbon ratio has been carried out for two different reformer concepts; one based on steam reforming (SR) and the other based on autothermal reforming (ATR).

Simulation results show that preheating of feed water and feed air has a positive effect on hydrogen efficiency. By applying high preheating temperatures hydrogen efficiencies of more than 80% can be achieved for both reformer concepts. However, thermal hydrogen efficiency is a rather theoretical parameter for evaluating reforming concepts for compact reformers in the transportation sector. Regarding small scale reformers for use in cars, trucks and ships it has to be considered that there is not enough external waste heat from other processes available to evaporate feed water, preheat feed fuel and feed air and supply the energy demand for the endothermic reforming reactions. We therefore strongly recommend to use the overall fuel processing efficiency  $\eta_{\text{FP}}$  (Eq. (16)) instead which also considers external energy demand for heating/cooling and electrical power for auxiliary devices.

Within this work the approach was to eliminate external heat demand by using only waste heat streams from within the system, avoiding any additional heat exchangers, thus keeping the system as simple as possible. Results show that the ATR concept with heat integration is competitive with the SR concept with heat integration in terms of fuel processing efficiency and overall system efficiency which is confirmed by studies of Ersoz et al. [13] and Salemme et al. [22]. Nevertheless, autothermal reforming is considered as the preferred option for reforming of bioethanol and biodiesel because of its lower system complexity and better dynamic behaviour.

#### References

- [1] C. Song, Catal. Today 77 (2002) 17–49.
- [2] T. Aicher, B. Lenz, F. Gschnell, U. Groos, F. Federici, L. Caprile, L. Parodi, J. Power Sources 154 (2006) 503–508.
- [3] S.J. Andreasen, S.K. Kær, Int. J. Hydrogen Energy 33 (2008) 4655–4664.
- [4] Q. Li, J.O. Jensen, R.F. Savinell, N.J. Bjerrum, Prog. Polym. Sci. 34 (2009) 449–477.
- [5] P.S. Nigam, A. Singh, Prog. Energy Combust. Sci. (2010) 003, doi:10.1016/j.pecs.2010.01.
- [6] A. Demirbas, Energy Convers. Manage. 50 (2009) 2239–2249.
- [7] G.R. Timilsina, A. Shrestha, Energy (2010) 023, doi:10.1016/j.energy.2010.08.
- [8] C.H. Bartholomew, R.J. Farrauto, Fundamentals of Industrial Catalytic Processes, second edition, Wiley, 2006.
- [9] A. Docter, A. Lamm, J. Power Sources 84 (1999) 194–200.
- [10] Q. Ming, T. Healey, L. Allen, P. Irving, Catal. Today 77 (2002) 51–64.
- [11] A. Cuttillo, S. Specchia, M. Antonini, G. Saracco, V. Specchia, J. Power Sources 154 (2006) 379–385.
- [12] I. Rosso, C. Galetti, G. Saracco, E. Garrone, V. Specchia, Appl. Catal. B: Environ. 48 (2004) 195–203.
- [13] A. Ersoz, H. Olgun, S. Ozdogan, J. Power Sources 154 (2006) 67–73.
- [14] P. Giunta, C. Mosquera, N. Amadeo, M. Laborde, J. Power Sources 164 (2007) 336–343.
- [15] A. Ersoz, H. Olgun, S. Ozdogan, C. Gungor, F. Akgun, M. Tiris, J. Power Sources 118 (2003) 384–392.
- [16] M. Benito, R. Padilla, J.L. Sanz, L. Daza, J. Power Sources 169 (2007) 123–130.
- [17] T.S. Christensen, Appl. Catal. A: Gen. 138 (1996) 285–309.
- [18] F.D. Alvarado, F. Gracia, Chem. Eng. J. (2010) 051, doi:10.1016/j.cej.2010.09.
- [19] T. Ioannides, J. Power Sources 92 (2001) 17–25.
- [20] J.A. Francesconi, D.G. Oliva, M.C. Mussati, P.A. Aguirre, Comput. Aided Chem. Eng. 27 (2009) 1791–1796.
- [21] S. Specchia, F.W.A. Tillemans, P.F. van den Oosterkamp, G. Saracco, J. Power Sources 145 (2005) 683–690.
- [22] L. Salemme, L. Menna, M. Simeone, Int. J. Hydrogen Energy 35 (2010) 3480–3489.

#### Glossary

- APU: auxiliary power unit  
 ATR: autothermal reforming  
 CR: CO<sub>2</sub> reforming  
 FID: flame ionization detector  
 GC: gas chromatography  
 HTPEM: high temperature polymer electrolyte membrane fuel cell  
 LHV: lower heating value  
 POX: partial oxidation  
 PEM: polymer electrolyte membrane fuel cell  
 S/C: steam to carbon ratio  
 SR: steam reforming  
 WGS: water gas shift